AN OVERVIEW OF LEG 172 LITERATURE[1]

L.D. Keigwin[2] and G.D. Acton[3]

INTRODUCTION

More than four years have passed since the completion of Ocean Drilling Program (ODP) Leg 172. Since then, the shipboard and other scientists have begun to complete their studies of cores recovered and data resulting from the cruise. The purpose of this paper is to give a brief overview of the main postcruise findings from papers published, in press, and submitted since the end of the cruise. Most of these are contained within this volume or are in a special issue of *Marine Geology,* edited by Leg 172 Co-Chief Scientist Dr. Domenico Rio. A smaller number of papers have been submitted to other journals. In addition, many of the research projects are still in their infancy and so a number of Leg 172 publications can be expected over the next few years.

Not surprisingly, the major themes of postcruise research are similar to the major themes identified by shipboard investigations. For convenience, the postcruise contributions to journal literature are grouped below according to the following disciplines: sedimentology and sediment chemistry, paleoceanography, and paleomagnetism.

A secondary purpose of this paper is to provide a current list of references that will help guide others in their search for Leg 172 literature. Realizing that our list will quickly become dated, we direct the readers to an Internet citations list at **http://www-odp.tamu.edu/publications/ pubs_ct.htm**. This list will continue to be updated by the ODP Publication Services staff to include future Leg 172 publications.

No overview of Leg 172 literature would be complete without at least mentioning the large amount of information available in the Leg 172 *Initial Results* volume (Keigwin, Rio, Acton, et al., 1998). Below, we borrow heavily from that volume in providing some key pieces of background information to aid the reader with this and other Leg 172 publications. Besides containing the observations and interpretations made by the shipboard scientists, a wealth of raw data are stored on CD-

ROMs in the back pocket of that volume. In addition, most of the data collected during the cruise have now been migrated to ODP's databases and are available on the Internet at http://www-odp.tamu.edu/database/, with logging data available at http://www.ldeo.columbia.edu/BRG/ODP/DATABASE/.

BACKGROUND

The main focus of Leg 172 was to recover thick Pliocene to Holocene sedimentary sequences from sediment drifts in the western North Atlantic that document rapid changes in climate and ocean circulation. These sediments were also thought to contain other valuable information, including high-resolution records of geomagnetic field behavior, records of mud wave formation and migration, sedimentary microstructures that reflect a combination of downslope and along-slope depositional processes, and geochemical signatures that might help assess the lateral distribution of the Blake hydrate field and the role of hydrates in diagenetic processes (Shipboard Scientific Party, 1998a).

Leg 172 succeeded in reaching all the coring objectives, with recovery of 5.8 km of core from 42 holes cored at 11 sites (Tables T1, T2). Two of the sites were located on the Carolina Rise, seven on the Blake-Bahama Outer Ridge (BBOR), one on the Bermuda Rise, and one in the Sohm Abyssal Plain (Figs. F1, F2). Sediments recovered at all 11 sites were younger than ~3 Ma. Ten of the sites were part of a depth transect, spanning 1300 to 4800 m water depth, that sought to document changes in the depth distribution of water masses since the latest Neogene (Fig. F3) (pp. 8–9 in Shipboard Scientific Party, 1998a). At each of these sites, three to eight holes were cored to ensure recovery of complete stratigraphic sections (Table T2). The sediments were dominated by alternations between clay-rich and carbonate-rich intervals generally related to glacial and interglacial periods, respectively (Fig. F4). Sedimentation rates at the nine deepest sites of the transect averaged 100–300 m/m.y. (10–30 cm/k.y.) over the past 1 m.y.

Besides observations made from core and logging studies, Leg 172 collected an atypically large amount of seismic and echo-sounder (3.5 kHz) data for an ODP cruise. The data, which are available from the ODP data bank at Lamont-Doherty Earth Observatory, were gathered along criss-crossing survey lines over each site, providing an abundance of information for subsurface investigations and regional correlation of sedimentary sequences.

SEDIMENTOLOGY AND SEDIMENT CHEMISTRY

To some extent, whether because of dissolution and precipitation or oxidation-reduction changes, all Leg 172 sedimentological patterns have a diagenetic signal that must be kept in mind. Çagatay et al. (in press) evaluated the broad diagenetic patterns across the Leg 172 depth transect based on their synthesis of interstitial water chemistry and sediment composition. They found that, in general, shallow water sites have greater sulfate reduction than deeper water sites because of higher iron content. From pore water analyses from eight of the sites along the depth transect, Borowski et al. (Chap. 3, this volume) found that dissolved carbon dioxide and methane pools are geochemically coupled through anaerobic methane oxidation and CO_2 reduction. They docu-

T1. Operations summary, Leg 172, p. 13.

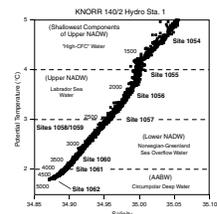T2. Drilling results, Leg 172, p. 14.

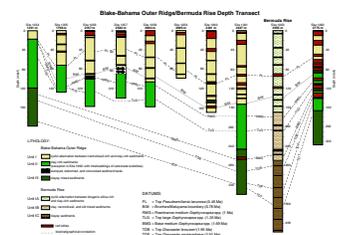F1. Map of the western North Atlantic showing Leg 172 sites, p. 9.
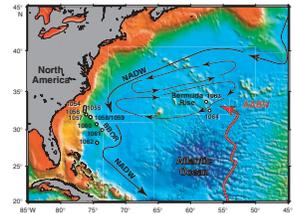
F2. Leg 172 site positions relative to bathymetry of the western North Atlantic, p. 10.
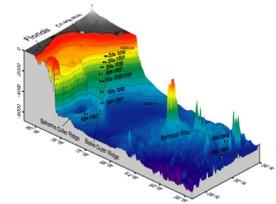
F3. Position of Leg 172 sites with respect to water masses in the western North Atlantic, p. 11.

F4. Generalized lithostratigraphy, biostratigraphy, and magnetostratigraphy of Leg 172 sites, p. 12.

mented large ^{13}C depletions at the sulfate/methane interface in dissolved CO_2 and methane. The similarity in levels of depletion of dissolved CO_2 and methane continue into the shallow methanogenic zone below the sulfate/methane interface and are inferred to result from the dissolved CO_2 being used as the substrate in the production of methane.

König et al. (Chap. 2, this volume) examined changes in the bulk sediment Fe(II)/Fe(III) ratio and in the distribution of iron among different minerals that result from storage after collection. Focusing their analysis on samples from Site 1062, they found that 24%–45% of the initial Fe(II) was oxidized to Fe(III) within only 6 months of refrigerated storage. Nearly the entire Fe(II) fraction was found to reside in structural iron in silicate mineral lattices. Thus, oxidation took place within the lattices. From these results, they suggested that modification of the magnetic signal during storage would be unlikely for Site 1062 sediments. They warned, however, that the reverse reactions (reduction diagenesis) likely occurred near the seafloor, which could have resulted in some chemical overprinting of the original magnetic signal as magnetite was progressively dissolved below the iron redox boundary. Diagenetic dissolution and redistribution of iron at and just below the seafloor could also affect the lithostratigraphic position of red lutites.

Giosan et al. (Chap. 6, this volume, submitted [N1]) and Giosan (2001) integrated reflectance spectra (color) with sediment chemistry for post–late Pliocene sediments. Part of their work illustrates how color reflectance can be used to estimate geochemical variations, particularly carbonate content. Their regression analysis provides a rapid and nondestructive means of estimating carbonate content that would otherwise require labor-intensive sampling and laboratory analysis. They also identified several key events in ocean climate history. First, a pulse of sediment delivery from the St. Lawrence system at the Pliocene/Pleistocene boundary indicates a Laurentide Ice Sheet influence on climate and ocean circulation at that time. For the past 900 k.y., sedimentation patterns in the western North Atlantic were dominated by the combination of sediment delivery and deep ocean circulation. Second, they infer that increased strength and deepening of the Western Boundary Undercurrent began between about 500 and 400 ka. Since that time, sediment delivery has increased during glacial stages, and in particular since marine isotope Stage (MIS) 6.

Complementing the color and sediment chemistry approach is the more geological methodology of Yokokawa (Chap. 7, this volume) and Yokokawa and Franz (in press). Based on an analysis of X-ray images, Yokokawa (Chap. 7, this volume) described sedimentary structures associated with episodic currents (turbidity currents and benthic storms) and more subtle sedimentary features associated with changes in color or magnetic susceptibility but not associated with distinct sedimentary structures in visual inspection of the core surfaces. Yokokawa and Franz (in press) analyzed sedimentary features, grain size variations, and anisotropy of magnetic susceptibility on sediments deposited during MIS 8 and 9. They found that the Deep Western Boundary Current (DWBC) must have strengthened and moved downward during interglacial 9.3 and interstadial 8.5. In contrast to Blake Outer Ridge sites, patterns of sedimentation were found to differ at the mud wave cored at Site 1062.

Two studies investigated the relationship between physical properties, sedimentary processes, and paleoceanography. Haskell (Chap. 4,

this volume) found that the sediments from Sites 1057 and 1061 have nearly isotropic magnetic susceptibility. He suggested this possibly indicates a circulation regime that was diffuse or at least currents that were too weak to effectively align oblate or elongate magnetic particles in the sediments at these sites. Dunbar (Chap. 5, this volume) examined why bulk density and *P*-wave velocity are in phase in some intervals but not in others within four Dansgaard-Oeschger (D-O) cycles that straddle the MIS 4/5 boundary (65–95 ka) in Hole 1063D (25–30 meters below seafloor [mbsf]) at the Bermuda Rise. Within this interval, density highs and lows are clearly associated with interstadial and stadial periods, respectively. In contrast, *P*-wave velocity can be high or low in the interstadials or stadials. Using X-ray diffraction, X-ray fluorescence, and particle size analyses, Dunbar showed that, as expected, calcite concentrations are highest in interstadials and aluminosilicate concentrations are highest in stadials, which explains much of the relationship between D-O cycles and density. More interestingly, he found that the composition of the aluminosilicates has subtle changes that correspond with the D-O cycles, with the ratios K_2O/Al_2O_3 and Al_2O_3/TiO_2 being low during interstadials and high during stadials. The *P*-wave velocity record does not, however, reflect simple fluctuations in the amount of calcite and aluminosilicates or in the composition of clay minerals. Instead, biogenic silica seems to play an important role, with high concentrations of biogenic silica correlating with intervals of high *P*-wave velocity, lower density, and increased particle sizes (increased volumes of silt and fine sand). Apparently, the biogenic silica forms a rigid framework that decreases density while being conducive to the transmission of acoustic waves. Hence, Dunbar concluded that the variable mixtures of calcite, aluminosilicates, and biogenic silica generate the distinct variations in physical properties as follows: intervals with high concentrations of calcite are characterized by high *P*-wave velocity and high density, intervals with high concentrations of aluminosilicates are characterized by low *P*-wave velocity and low density, and intervals with high concentrations of biogenic silica are characterized by high *P*-wave velocity and low density.

Winter (Chap. 8, this volume) cataloged the types and abundances of diatoms in the upper 30 m of Hole 1063D. Like Dunbar (Chap. 5, this volume), she found that high diatom abundance correlates with density lows in the 25–30 mbsf range and she confirmed that this relationship continues further uphole. She also observed diatom species that are restricted ecologically to coastal or littoral waters, requiring that they have been transported to Site 1063 by currents. She suggested the uphole decrease in abundance of these species may indicate changes in currents or in the water masses that reach the site over time.

During Leg 172, we were puzzled by the presence of a waxy, yellowish brown amorphous material, which occupied vertical fractures in drilling biscuits in two intervals (265.5–270.0 and 347.44–349.09 mbsf) in Hole 1063B. Eglinton and Whelan (Chap. 1, this volume) solved this puzzle by analyzing samples of the material with flash pyrolysis gas chromatography mass spectrometry. They concluded that the material was neither derived from petroleum nor geochemically related to thermally mature hydrocarbons. Instead, they suggested it is possibly a fragment of an algal mat or some other immature biologically derived material.

Flood and Giosan (submitted [N2]) focused exclusively on the multiple holes at Site 1062 along the crest of a mud wave near the Bahama Outer Ridge. They combined lithostratigraphy and acoustic stratigra-

phy to determine the history of wave migration and, hence, current speed. Wave migration was pronounced during the interval 5 to 1 Ma, but it has been slower since 1 Ma. During deglacial episodes of the past 0.5 m.y., there may have been no wave migration at all. This could reflect sluggish deep ocean circulation as ice sheets melted and suppressed ocean convection.

PALEOCEANOGRAPHY

With the higher resolution of paleoceanographic studies at sites such as those collected during Leg 172, the more important becomes the stratigraphic correlations among sites and their chronology. Grutzner et al. (in press) have provided an important baseline for study of these sites through their development of age models based on tuning estimated carbonate content (from sediment lightness) to the orbital parameters precession and obliquity. They found that sites tend to group into those from shallow locations where precession dominates carbonate content (2200–3000 m) and deeper sites where obliquity dominates (3000–4800 m). Time series analyses of the resulting age series of carbonate reveal several significant periods in the range 12 to 1.5 k.y. Although these results are preliminary and will be improved upon as more oxygen isotope data become available, recognition of periodicities as short as 1500 yr by Grutzner et al. (in press) shows the promise of Leg 172 sites for high-resolution studies of the ocean and climate.

Using stable isotopes, Bianchi et al. (in press) established the bathymetric gradients between the deep Blake Outer Ridge (Site 1060) and the Bahama Outer Ridge (Site 1062) from MIS 5e–5d. They found no $\delta^{13}C$ contrast, and high $\delta^{13}C$ during MIS 5e, which indicates strong Lower North Atlantic Deep Water (LNADW) flow over both sites. A $\delta^{13}C$ gradient developed late in MIS 5e and early in MIS 5d, but by ~113 ka both locations were overlain by a nutrient-rich water mass. In contrast to $\delta^{13}C$, the sortable silt parameter indicates significant and coherent variability at both sites throughout the MIS 5e–5d interval.

Oppo et al. (2001) also concentrated on MIS 5e, but at Site 1059. They compared stable isotope results there with those from two locations in the subpolar North Atlantic (including ODP Site 980). At each location they found millennial-scale variability in sea-surface temperature (SST) proxies, despite the minimum in ice volume. However, as reported by Bianchi et al. (in press) for deeper sites, they found no strong geochemical evidence for NADW change during the last interglacial.

Site 1059 is also featured in a paper by Hagen and Keigwin (in press). All stadial–interstadial changes in climate recognized for MIS 3 in Greenland ice are evident at this site. SST oscillations were as large as 4°C, based on $\delta^{18}O$ of *Globigerinoides ruber,* which also typically varies between 20% and 40% of the planktonic fauna. *Neogloboquadrina pachyderma* (left coiling) occasionally exceeds 2% of the fauna during the coldest episodes of MIS 2 and 3. In general, there is a relationship between interstadial climate and high production of NADW (high $\delta^{13}C$). However, notable exceptions to this pattern occur during the long interstadials 12 and 14 (~45 and 52 ka). At those times, there seems to be a lag of >1 k.y. between interstadial warming and increased NADW flow.

Keigwin (Chap. 9, this volume) assessed the significance of red sediments (red lutites) through an oxygen isotope study of select intervals within MIS 1 to 6 at Sites 1054, 1055, and 1063. For the deeper Sites

1055 and 1063, maxima in planktonic values coincided with intervals with redder sediments, indicating a connection between colder SST and deep circulation that transports the red lutites from their source in eastern Canada. Site 1054, which is only 24 km away from Site 1055 but is 500 m shallower, has a notable absence of reddish sediment. From measurements of planktonic $\delta^{18}O$ through the last glacial maximum (LGM) interval at these two sites, Keigwin noted lower values at Site 1054 than at Site 1055. He suggested this could result from higher SST at Site 1054, possibly related to the proximity of this site to the core of the Gulf Stream. He surmised that the lack of red sediment at Site 1054 may indicate that the shallowest components of the DWBC were deeper than Site 1054 during the LGM.

The group of Thunell, Poli, and Rio investigated the interval MIS 9–12. Thunell et al. (in press) used carbonate stratigraphy to identify particular time slices for paleohydrographic reconstruction within the interval MIS 10–12. They found nutrient depletion in MIS 12 above 2000 m, whereas MIS 11 was similar to today (with high $\delta^{13}C$ between 3500 and 2000 m and lower $\delta^{13}C$ below 3500 m). In general, MIS 10 and 12 were similar. This group also conducted a time series study of the same time interval at Bermuda Rise Site 1063 (Poli et al., 2000). Millennial-scale variability is typical in both MIS 12 and 11. MIS 12 had interstadials every several thousand years and traces of ice rafting during stadial events. Interstadial events in MIS 11 (high carbonate and high NADW flow) were found to correlate with warm events in the Vostok ice core.

Franz and Tiedemann (in press) sampled MIS 8–10 at better than 1-k.y. resolution for stable isotope and sedimentology studies. From MIS 9 to 8.5, waters as deep as 3 km were well ventilated, but during the glacial epochs before and after AABW shoaled to 2200 m. Leg 172 sites recorded the subtle interplay between source of sediment, redistribution by DWBC, varying corrosiveness of bottom waters, and carbonate dissolution driven by organic carbon fluxes.

PALEOMAGNETISM

One of the striking results of Leg 172 was the discovery of numerous geomagnetic excursions that occur within the Brunhes Chron (0–780 ka). Lund et al. (1998) documented 14 plausible excursions from shipboard results. The term plausible was used to denote excursions that gave virtual geomagnetic poles (VGPs) deviating by more than 45° from Earth's spin axis and that occurred in at least four different holes at two or more sites. They noted that not only was the number of excursions much larger than previously thought, the percentage of time that the Brunhes paleomagnetic field was in an excursional state was much longer than previous observations indicated or models predicted. The total time the geomagnetic field was in an excursional state possibly represented more than 20% of the past 780 k.y. Lund et al. (Chap. 10, this volume) reiterated these basic findings, although they also further probed the paleomagnetic signal of the sediments with detailed U-channel and discrete sample measurements. They confirmed the directional changes for 12 of the 14 plausible excursions, suggesting that one of the directional deviations that occurred in MIS 3 (Excursion 3α) and another in MIS 5 (Excursion 5α) should no longer be considered true excursions. The U-channel measurements also resulted in the identification of one new excursion in MIS 17.

More detailed analyses of individual excursions have also been conducted. Lund et al. (Chap. 11, this volume) explored the variability of the geomagnetic field in MIS 3 at Sites 1061, 1062, and 1063. The younger of the two MIS 3 excursions, referred to as Excursion 3α, was shown to have less directional variability than was apparent in the shipboard split-core paleomagnetic measurements. The older MIS 3 excursion, referred to as Excursion 3β, was interpreted to be the Laschamp Excursion. They also showed that the secular variation of the geomagnetic field before and after this excursion could be correlated between sites >1000 km apart. Williams et al. (submitted [N3]) examined three excursions in MIS 7 and 8. One, referred to as Excursion 7α, occurs at ~190 ka and correlates well with known events on land in North America and in the Pacific region. The two other excursions are associated with changes in sediment characteristics such as carbonate content. Although there is no obvious relationship between the sediment changes and the magnetic changes, these authors are less certain that the magnetic changes in those samples reflect real magnetic field behavior than they are for the ~190-ka event.

Acton et al. (submitted [N4]) evaluated magnetic artifacts in ODP piston cores. Besides the ubiquitous isothermal remanent magnetizations imparted by the drill string, which are easy to recognize and remove, they noted the existence of more subtle overprints that result from shearing of the sediment as the corer penetrates. They developed a model to predict the size and sense of the deflection of the paleomagnetic remanence. This model successfully accounts for the difference in remanence between split-core data, which contain shear biases, and U-channel data from the center of a core where there is no shear.

Finally, Clement et al. (submitted [N5]) took advantage of high sedimentation rates to examine the reversals associated with the Cobb Mountain Subchron on the Bermuda Rise. U-channel samples were analyzed from two holes at Site 1063 to identify and remove artifacts. The stacked results compare favorably with the path taken by the virtual geomagnetic pole as measured in other sites, and they indicate that the transitional magnetic field was probably dipolar throughout the reversal.

REFERENCES

Bianchi, G.G., Vautravers, M., and Shackleton, N.J., in press. Deep flow variability under apparently stable North Atlantic Deep Water production during the last interglacial of the sub-tropical NW Atlantic. *Paleoceanography.*

Çagatay, M.N., Borowski, W.S., and Ternois, Y.G., in press. Diagenesis of Quaternary sediments in the western North Atlantic. *Mar. Geol.*

Franz, S.O., and Tiedemann, R., in press. Depositional changes along the Blake-Bahama Outer Ridge deep water transect during marine isotope Stages 8 to 10—links to the Deep Western Boundary Current. *Mar. Geol.*

Giosan, L., 2001. The use of sediment color in paleoceanography: Pliocene–Pleistocene sedimentation in the western North Atlantic. [Ph.D. dissert.] State Univ. New York, Stony Brook.

Grutzner, J., Giosan, L., Franz, S.O., Tiedemann, R., Cortijo, E., Chaisson, W.P., Flood, R.G., Hagen, S., Keigwin, L.D., Poli, S., Rio, D., and Williams, T., in press. Astronomical age models for Pleistocene drift deposits from the western North Atlantic (ODP Sites 1055 to 1063). *Mar. Geol.*

Hagen, S., and Keigwin, L.D., in press. Sea surface temperature variability and deep water reorganization in the North Atlantic during isotope Stage 2–4. *Mar. Geol.*

Keigwin, L.D., Rio, D., Acton, G.D., et al., 1998. *Proc. ODP, Init. Repts.,* 172 [CD-ROM]. Available from: Ocean Drilling Program, Texas A&M University, College Station, TX 77845-9547, U.S.A.

Lund, S.P., Acton, G., Clement, B., Okada, M., and Williams, T., 1998. Initial paleomagnetic results from ODP Leg 172: high resolution geomagnetic field behavior for the last 1.2 Ma. *Eos,* 79:178–179.

Oppo, D.W., Keigwin, L.D., McManus, J.F., and Cullen, J.L., 2001. Persistent suborbital climate variability in marine isotope Stage 5 and Termination II. *Paleoceanography,* 16:280–292.

Poli, M., Thunell, R., and Rio, D., 2000. Millennial-scale changes in North Atlantic deep water circulation during marine isotope Stages 11–12: linkage to Antarctic climate. *Geology,* 28:807–810.

Shipboard Scientific Party, 1998a. Introduction. *In* Keigwin, L.D., Rio, D., Acton, G.D., et al., *Proc. ODP, Init. Repts.,* 172, 7–12 [CD-ROM]. Available from: Ocean Drilling Program, Texas A&M University, College Station, TX 77845-9547, U.S.A.

————, 1998b. Summary. *In* Keigwin, L.D., Rio, D., Acton, G.D., et al., *Proc. ODP, Init. Repts.,* 172, 311–324 [CD-ROM]. Available from: Ocean Drilling Program, Texas A&M University, College Station, TX 77845-9547, U.S.A.

Thunell, R., Poli, M.S., and Rio, D., in press. Changes in intermediate and deep water mass properties in the western North Atlantic during isotope Stages 11–12: results from ODP leg 172. *Mar. Geol.*

Yokokawa, M., and Franz, S.O., in press. Changes in grain size and magnetic fabric at the Blake-Bahama Outer Ridge during the late Pleistocene (marine isotope Stages 8–10). *Mar. Geol.*

Figure F1. Map of the western North Atlantic showing the Leg 172 site locations on the Carolina Slope (Sites 1054 and 1055), the Blake-Bahama Outer Ridge (BBOR) (Sites 1056–1062), the northeast Bermuda Rise (Site 1063), and the Sohm Abyssal Plain (Site 1064). Imposed on top of this are schematic circulation patterns, including the North Atlantic Deep Water (NADW) (thick black lines), Antarctic Bottom Water (AABW) (thick shaded line), and gyre currents (thin black lines).
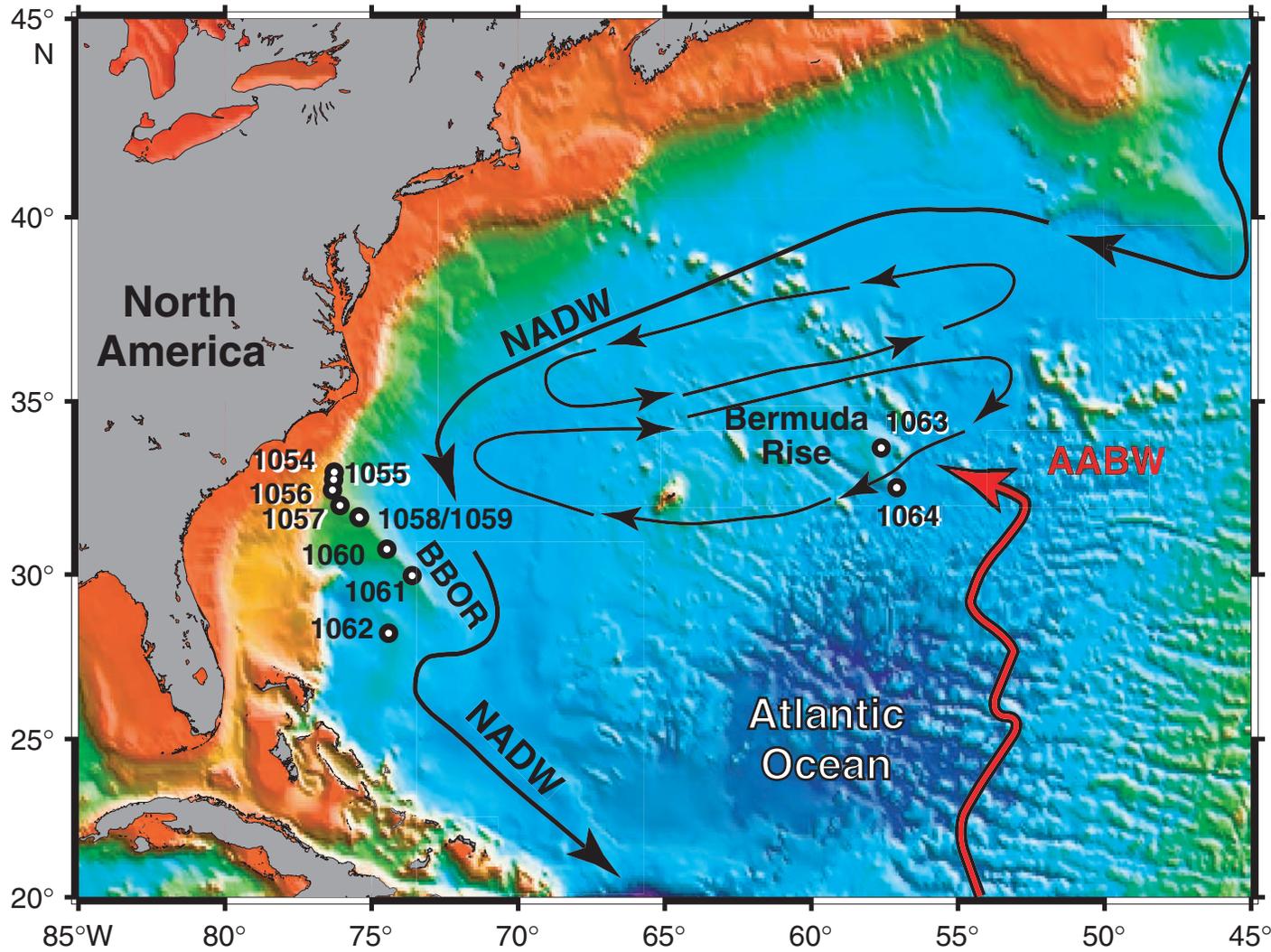
Figure F2. Leg 172 site locations illustrating their positions relative to bathymetry of the western North Atlantic (from the frontispiece of Keigwin, Rio, Acton, et al., 1998).
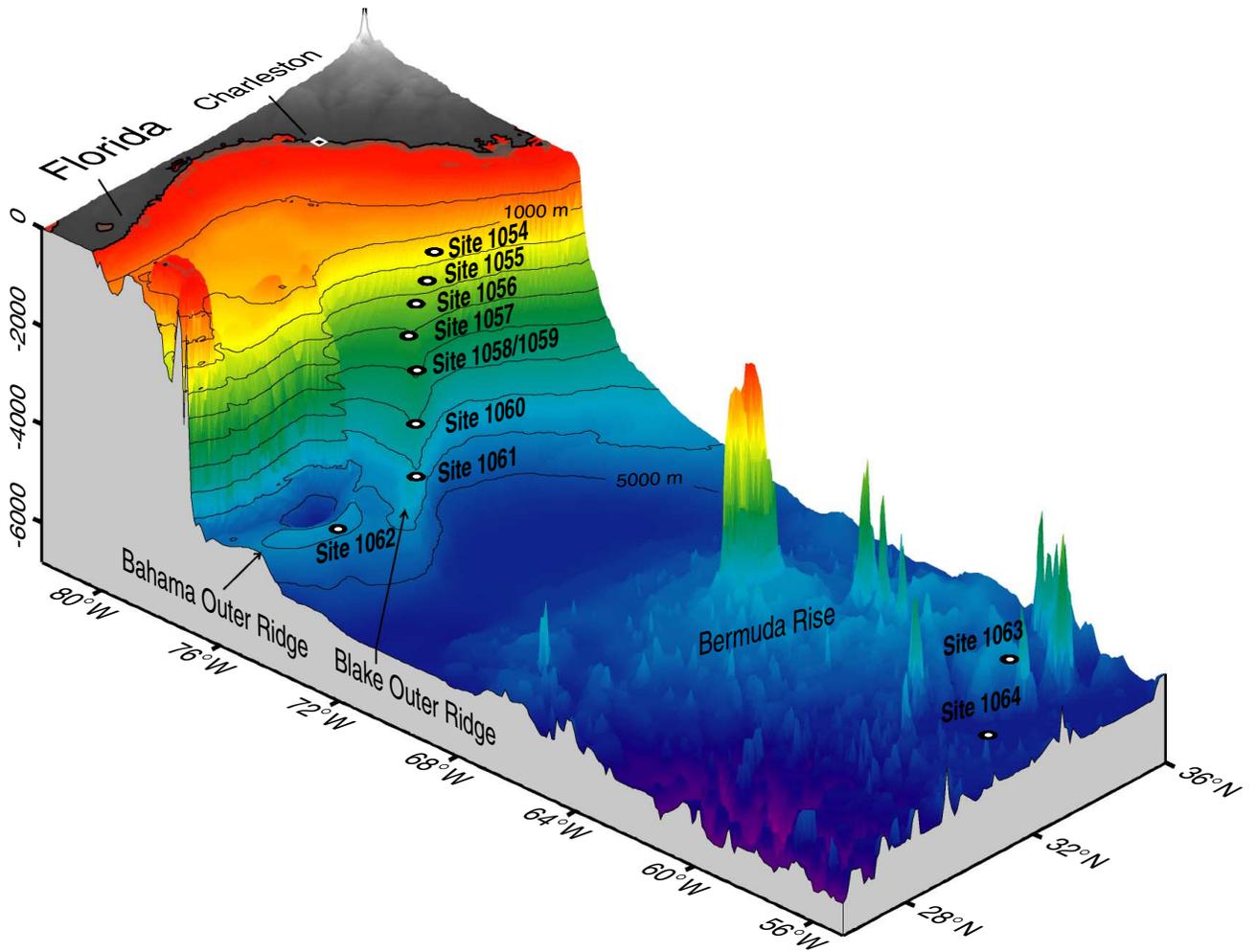
Figure F3. Position of Leg 172 BBOR sites with respect to water masses in the western subtropical North Atlantic. Water depths are indicated every 500 m along the temperature/salinity plot. Sites were chosen so that at least one lies within each modern water mass and one lies at the boundary between water masses. This depth distribution of sites is required to monitor the most likely changes in water masses and their boundaries through the late Neogene. *KNORR* 140/2 Hydro Sta. 1 refers to the site survey cruise and station number that were used to collect the data. "High-CFC" indicates the shallowest components of North Atlantic Deep Water (NADW) that originate in and near Labrador Sea and can be traced using chlorofluorcarbons. AABW = Antarctic Bottom Water (modified from fig. 3 in Shipboard Scientific Party, 1998a).

KNORR 140/2 Hydro Sta. 1
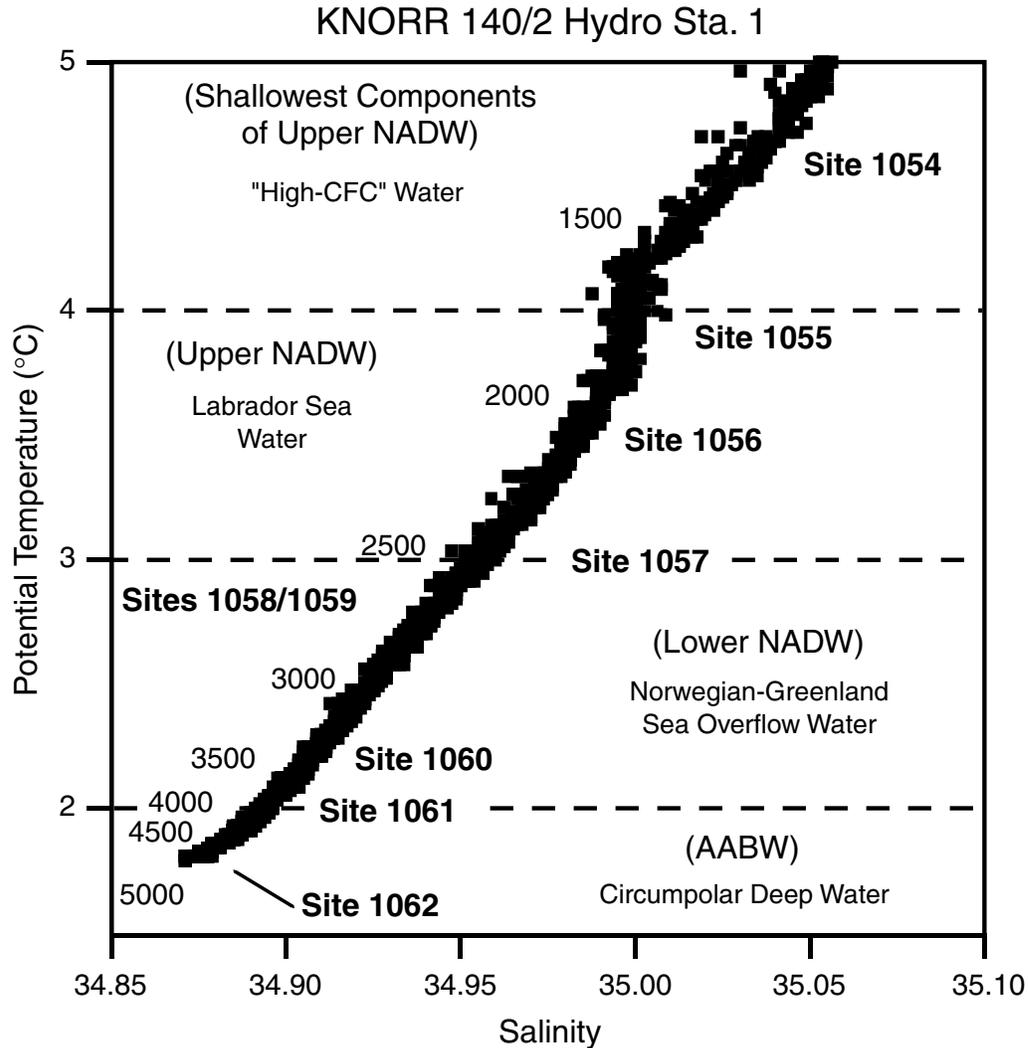
Figure F4. Generalized lithostratigraphy, biostratigraphy, and magnetostratigraphy of Leg 172 sites, except Site 1064. Note the similar sequence of units at all sites. As discussed in the text, this most likely reflects coherent variation of sediment distribution by deep ocean currents basinwide through the late Pliocene and Pleistocene (modified from fig. 2 in Shipboard Scientific Party, 1998b).

Blake-Bahama Outer Ridge/Bermuda Rise Depth Transect

LITHOLOGY:

Blake-Bahama Outer Ridge

Unit I — cyclic alternation between nannofossil-rich and clay-rich sediments

Unit II — clay-rich sediments (exception in Site 1062: with interbeddings of carbonate turbidites)

— slumped, deformed, and convoluted sediment beds

Unit III — clayey mixed sediments

Bermuda Rise

Unit IA — cyclic alternation between biogenic silica-rich and clay-rich sediments

Unit IB — clay, nannofossil, and silt mixed sediments

Unit IC — clayey sediments

— red lutites

- - - - biostratigraphical correlation

——— magnetostratigraphic correlation

DATUMS:

PL = Top *Pseudoemiliania lacunosa* (0.46 Ma)
B/M = Brunhes/Matuyama boundary (0.78 Ma)
RMG = Reentrance medium *Gephyrocapsa* spp. (1 Ma)
TLG = Top large *Gephyrocapsa* spp. (1.25 Ma)
BMG = Base medium *Gephyrocapsa* spp. (1.69 Ma)
TDB = Top *Discoaster brouweri* (1.95 Ma)
TDP = Top *Discoaster pentaradiatus* (2.52 Ma)
TDT = Top *Discoaster tamalis* (2.83 Ma)

Table T1. Operations summary, Leg 172.

Total days (14 February 1997 to 16 April 1997):	60.06
Total days in port + 6-hr clock advance:	6.18
Total days under way:	15.90
Total days on site:	37.98
Breakdown of site operations (days):	
Coring	24.86
Drilling	<0.01
Tripping time	7.93
Stuck pipe/hole trouble	0.30
Logging/downhole science	1.95
Mechanical repair time (contractor)	1.14
Reentry time	0.00
Waiting on weather	0.75
Other:	1.04
Total distance traveled (nmi):	4405
Average speed of transit (kt):	11
Number of sites:	11
Number of holes:	42
Number of cores attempted:	623
Total interval cored (m):	5688.8
Total core recovery (m):	5765.3
Core recovery (%):	101.3
Total interval drilled (m):	9.6
Total penetration (m):	5698.4
Maximum penetration (m):	418.4
Minimum penetration (m):	9.5
Maximum water depth (m):	5568.3
Minimum water depth (m):	1291.3

Table T2. Leg 172 drilling results.

Hole	Latitude	Longitude	Water depth (m)	Number of cores	Interval cored (m)	Core recovered (m)	Recovery (%)	Total penetration (m)
1054A	33°00.0001′N	76°16.9996′W	1291.3	22	200.00	182.55	91.3	200.00
1054B	32°59.9850′N	76°16.9999′W	1293.6	12	103.20	106.29	103.0	103.20
1054C	32°59.9676″N	76°16.9995′W	1294.7	13	101.90	104.55	102.6	101.90
		Site 1054 totals:		47	405.10	393.39	97.1	405.10
1055A	32°47.0418′N	76°17.1703′W	1798.7	1	9.50	9.82	103.4	9.50
1055B	32°47.0406′N	76°17.1790′W	1797.7	14	128.00	137.99	107.8	128.00
1055C	32°47.0562′N	76°17.1798′W	1797.7	14	120.80	126.10	104.4	120.80
1055D	32°47.0711′N	76°17.1792′W	1798.6	14	129.10	136.99	106.1	129.10
1055E	32°47.0925′N	76°17.1799′W	1797.7	2	18.00	18.48	102.7	18.00
		Site 1055 totals:		45	405.40	429.38	105.9	405.40
1056A	32°29.0995′N	76°19.8025′W	2166.7	1	9.50	9.98	105.1	9.50
1056B	32°29.1018′N	76°19.7988′W	2166.6	17	155.60	171.81	110.4	155.60
1056C	32°29.1105′N	76°19.8113′W	2166.9	17	154.80	166.25	107.4	154.80
1056D	32°29.1215′N	76°19.8253′W	2166.4	13	121.80	132.46	108.8	121.80
		Site 1056 totals:		48	441.70	480.50	108.8	441.70
1057A	32°01.7507′N	76°04.7527′W	2583.7	14	131.00	141.67	108.1	131.00
1057B	32°01.7317′N	76°04.7538′W	2584.5	15	136.70	145.08	106.1	136.70
1057C	32°01.7141′N	76°04.7546′W	2583.2	8	73.50	77.46	105.4	73.50
		Site 1057 totals:		37	341.20	364.21	106.7	341.20
1058A	31°41.4153′N	75°25.8049′W	2984.5	16	152.00	164.56	108.3	152.00
1058B	31°41.4022′N	75°25.8038′W	2984.0	17	158.00	166.00	105.1	158.00
1058C	31°41.3861′N	75°25.8014′W	2984.0	18	164.00	173.81	106.0	164.00
		Site 1058 totals:		51	474.00	504.37	106.4	474.00
1059A	31°40.4610′N	75°25.1270′W	2985.4	11	98.80	105.49	106.8	98.80
1059B	31°40.4528′N	75°25.1121′W	2985.2	10	92.20	95.91	104.0	92.20
1059C	31°40.4421′N	75°25.0983′W	2984.7	10	95.00	100.54	105.8	95.00
		Site 1059 totals:		31	286.00	301.94	105.6	286.00
1060A	30°45.5971′N	74°27.9897′W	3481.2	18	170.10	177.74	104.5	170.10
1060B	30°45.5849′N	74°27.9887′W	3480.8	14	129.90	134.23	103.3	129.90
1060C	30°45.5682′N	74°27.9896′W	3481.2	14	126.50	130.78	103.4	126.50
		Site 1060 totals:		46	426.50	442.75	103.8	426.50
1061A	29°58.4976′N	73°35.9929′W	4046.6	37	350.30	298.20	85.1	350.30
1061B	29°58.5172′N	73°35.9914′W	4043.6	1	9.50	9.82	103.4	9.50
1061C	29°58.5154′N	73°35.9923′W	4036.8	18	166.80	174.61	104.7	166.80
1061D	29°58.5326′N	73°35.9900′W	4038.4	22	180.00	194.95	108.3	180.00
1061E	29°58.5563′N	73°35.9933′W	4035.7	2	18.90	19.53	103.3	18.90
		Site 1061 totals:		80	725.50	697.11	96.1	725.50
1062A	28°14.7819′N	74°24.4192′W	4763.3	20	180.70	181.24	100.3	180.70
1062B	28°14.7888′N	74°24.4204′W	4763.0	26	239.00	239.08	100.0	248.60
1062C	28°14.7954′N	74°24.4163′W	4760.6	14	132.90	134.56	101.2	132.90
1062D	28°14.7998′N	74°24.4157′W	4760.2	9	81.80	82.66	101.1	81.80
1062E	28°14.7653′N	74°25.0552′W	4774.0	23	208.80	203.72	97.6	208.80
1062F	28°14.7710′N	74°25.0651′W	4773.7	9	83.10	83.77	100.8	83.40
1062G	28°14.7548′N	74°24.6218′W	4747.5	1	9.30	9.27	99.7	9.30
1062H	28°14.7537′N	74°24.6204′W	4745.3	7	63.50	65.29	102.8	63.50
		Site 1062 totals:		109	999.10	999.59	100.0	1008.70
1063A	33°41.2043′N	57°36.8979′W	4583.5	45	418.40	400.34	95.7	418.40
1063B	33°41.1885′N	57°36.8982′W	4583.0	38	351.60	341.95	97.3	351.60
1063C	33°41.1808′N	57°36.9028′W	4584.1	24	212.70	204.39	96.1	212.70
1063D	33°41.1717′N	57°36.9067′W	4584.3	19	173.10	176.54	102.0	173.10
		Site 1063 totals:		126	1155.80	1123.22	97.2	1155.80
1064A	32°32.7199′N	57°04.5876′W	5568.3	3	28.50	28.83	101.2	28.50
		Site 1064 totals:		3	28.50	28.83	101.2	28.50
		Leg 172 totals:		623	5688.80	5765.29	101.3	5698.40

CHAPTER NOTES*

N1. Giosan, L., Flood, R.G., Aller, R.C., Grutzner, J., Mudie, P., submitted. Paleoceanographic significance of sediment color on western North Atlantic drifts (ODP Leg 172). *Mar. Geol.*

N2. Flood, R.G., and Giosan, L., submitted. Migration history of an abyssal mud wave on the Bahama Outer Ridge. *Mar. Geol.*

N3. Williams, T., Lund, S., Acton, G., Clement, B., Okada, M., and Hastedt, M., submitted. Sedimentary records of three geomagnetic excursions during δ^{18}O Stages 7 and 8, from the Blake Ridge, North Atlantic, ODP Leg 172. *Earth Planet. Sci. Lett.*

N4. Acton, G.D, Okada, M., Clement, B.M., Lund, S.P., and Williams, T., submitted. Drilling induced paleomagnetic overprints in ocean sediment cores and their relationship to shear deformation caused by piston coring. *J. Geophys. Res.*

N5. Clement, B.M., Yang, Z., Acton, G.D., Lund, S.P., Okada, M., Williams, T., submitted. Records of the Cobb Mountain Subchron from the Bermuda Rise (ODP Leg 172). *Earth Planet. Sci. Lett.*

*Dates reflect file corrections or revisions.